Lifetime Extension of Lithium-ion Batteries with Low-Frequency Pulsed Current Charging

Huang, Xinrong; Liu, Wenjie; Meng, Jinhao ; Li, Yuanyuan; Jin, Siyu; Teodorescu, Remus; Stroe, Daniel-Ioan

Published in:
I E E E Journal of Emerging and Selected Topics in Power Electronics

DOI (link to publication from Publisher):
10.1109/JESTPE.2021.3130424

Publication date:
2023

Document Version
Accepted author manuscript, peer reviewed version

Lifetime Extension of Lithium-ion Batteries with Low-Frequency Pulsed Current Charging

Xinrong Huang, *Student Member, IEEE*, Wenjie Liu, *Student Member, IEEE*, Jinhao Meng, *Member, IEEE*, Yuanyuan Li, Siyu Jin, Remus Teodorescu, *Fellow, IEEE*, and Daniel-Ioan Stroe, *Member, IEEE*

***Abstract*—The pulsed current has been proposed to achieve fast charging and extend the lifetime of Lithium-ion (Li-ion) batteries. However, the optimal condition of the pulsed current is still inconclusive in previous studies. This paper experimentally investigated the effect of the low-frequency Positive Pulsed Current (PPC) charging on the lifetime and charging performance of Li-ion batteries. A two-stage degradation model of Li-ion batteries is developed to determine the inhibitory effect of the PPC on degradation mechanisms at different aging stages. Moreover, the changes in the Internal Resistance (IR) and the Incremental Capacity (IC) curve are provided to thoroughly explore the effects of the PPC on the degradation of Li-ion batteries. Compared with the traditional Constant Current (CC) charging, the lifetime, maximum rising temperature, and energy efficiency of the Li-ion batteries that were cycled by the PPC charging are improved by 81.6%, 60.5%, and 9.1%, respectively, after 1000 cycles. Therefore, low-frequency PPC charging should be considered as a promising charging strategy for Li-ion batteries.**

***Index Terms*—Lifetime extension, Lithium-ion (Li-ion) battery, pulsed current charging, frequency**

I. Introduction

To establish a friendly ecological environment, the major economies worldwide have provided a strong support policy on the electrification o f r oad t raffic [1]. Many countries have formulated a series of policies to encourage EV development, e.g., increasing investment in infrastructure and implementing tax exemptions for manufacturers [2], [3]. Lithium-ion (Li-ion) batteries play an important role among the energy storage technologies due to their high energy and power density, long lifetime, and low self-discharge rate [4], [5], which makes them suitable for EV applications. However, nowadays, EVs take more time to replenish energy when compared with the time that traditional internal combustion engine vehicles need for fueling (i.e., few minutes). Therefore, it is essential to develop fast charging technology for Li-ion batteries in EVs. Constant Current-Constant Voltage (CC-CV) charging method is used to determine the battery capacity [6], [7]. According to the experimental result in [8], the CV phase of the CC-CV charging contributes to 22% of the discharging capacity but accounts for 48% of the charging time. Therefore, the Constant Current (CC) charging is regarded as a practical method to charge the batteries, especially pursuing a balance between the charging time and discharging capacity [9]. To further improve the charging speed, a simple method is to increase the current rate of the CC charging; however, this will, in turn, reduce the available discharging capacity and increase the battery temperature, which shortens the battery lifetime [10]. Therefore, achieving a trade-off between the charging speed and lifetime has been a significant target of numerous studies investigating advanced charging strategies.

To optimize the charging process, various Multi-Stage Constant Current (MSCC) charging methods have been proposed to achieve different charging targets, e.g., fast charging and cell temperature control [11]–[13]. However, the MSCC charging method needs a complex controller to decide the turning point of adjacent stages during the charging process, which usually requires accurate SOC and SOH estimation. In recent years, SOC and SOH estimations based on machine learning have developed rapidly, and most of them were developed based on data analysis [14]–[17]. Even though, few of them further investigated the effect of the proposed MSCC charging methods on the battery lifetime. The Sinusoidal-Ripple Current (SRC) charging method was proposed to improve the charging performance for Li-ion batteries in [18]. Moreover, the SRC charging with optimal frequency can extend the battery lifetime by 16.1% compared with the CC-CV charging [18]. However, compared with the CC charging, the SRC charging shows no significant effect on the battery lifetime when the current frequency is between 1 Hz and 1 kHz [19]. The pulsed current charging technique has been proposed to improve the battery lifetime and charging performance [20]–[23]. However, the optimal condition of those pulsed current charging for Li-ion battery lifetime extension still needs to be investigated due to the inconclusive aging effect reported in the avaliable literature. Therefore, this work will focus on one of the pulse current charging methods, i.e., Positive Pulsed Current (PPC) charging, to obtain its effect on the lifetime of Li-ion batteries.

The paper is structured as follows. The background of the pulsed current charging and the degradation mechanism of the Li-ion batteries are introduced in section II. The experimental methods are presented in section III. The experimental results and analysis are provided in section IV. The conclusions are given in section V.

This work was supported in part by the China Scholarship Council under grant CSC201806290017, in part by Sichuan Science and Technology Program under grant 2021YJ0063, and in part by the National Natural Science Foundation of China under grant 52107229.

Corresponding author: W. Liu (wie@et.aau.dk).

X. Huang, W. Liu, S. Jin, R. Teodorescu, and D. Stroe are with the Department of Energy Technology, Aalborg University, Aalborg 9220, Denmark.

J. Meng is with the College of Electric Engineering, Sichuan University, Chengdu 610065, China.

Y. Li is with the College of electrical engineering, Southwest Minzu University, Chengdu 610041, China.

II. Background

A. Pulsed Current Charging

There are four basic pulsed current charging modes, i.e., Negative Pulsed Current (NPC), Alternating Pulsed Current (APC), Pulsed Current-Constant Current (PCCC), and PPC, respectively [24]. The NPC mode is the constant current with periodic negative pulses and relaxation time, which can eliminate the concentration polarization and improve the battery lifetime by 128.6% compared to the CC-CV charging [20]. In [21], multiple sets of experiments were designed to investigate the effect on the Li-ion battery lifetime of the NPC-CV charging with different amplitude and number of negative pulses, which reveals that the NPC-CV charging with a low amplitude and few negative pulses has a positive impact on the battery lifetime [21]. In [25], the NPC-CV charging at 0.023 Hz and 0.046 Hz can improve the battery lifetime by around 17.1% when compared to the CC-CV charging. However, the charging rate of the NPC-CV is lower than that of the CC-CV charging due to the discharging pulses during the charging process [21]. The APC mode is the constant current with periodic negative pulses [24]. The APC-CV charging has no significant effect on battery charging performance in terms of charging and discharging capacity and energy [26]. Moreover, similar to the NPC charging, the charging rate of the APC is affected by the discharging pulses during the charging process. The PPC mode is the constant current with periodic relaxation time. In [27], the PPC-CV charging at a frequency of 1 kHz has no significant impact on battery lifetime, while at 50 Hz and 100 Hz can result in a faster capacity fade compared with the CC-CV charging during cycling. In [22], it was shown that the PPC charging at a frequency of 12 kHz can extend the battery lifetime by 100 cycles compared with the CC-CV charging. The PCCC mode is the positive pulsed current followed by a constant current. The difference between the PCCC and the PPC is that the current during the relaxation time is not zero but a constant current. In [28], the effect of PCCC on battery lifetime was investigated at frequencies of 1 Hz and 25 Hz. The PCCC charging has a similar rate of capacity fade compared with the CC-CV charging, but the capacity utilization using PPC charging is the only 80% of CC-CV charging [28]. In our previous work, various pulsed current modes, i.e., PPC, PCCC, APC, NPC, and SRC, were considered to study their effects on battery charging performance [29]. The results show that the pulsed current can not impact the charging speed but result in an increase in the maximum rising temperature of the battery cell compared with the CC charging [29]. In [8], [30], similar conclusions as [29] have been reported, i.e., the PPC and SRC charging can not affect the charging speed but results in a higher rising temperature when compared with the CC charging.

Table I summarized the effect of various pulsed current on Li-ion batteries' lifetime in previous studies. According to the aforementioned studies, the NPC charging can extend the battery lifetime but lower the charging rate; the PPC charging is a possible way to improve the battery lifetime without affecting the charging rate, but the effect of the frequency of the PPC charging still needs to be explored. The optimal charging frequency is firstly proposed in [18]. The authors of [18] believe that the optimal frequency point f_{min} is where the battery cell can return the minimum impedance, which can be obtained by the electrochemical impedance spectroscopy (EIS) test. This opinion is supported by [22] and [23], who experimentally verified the PPC charging at the frequency of f_{min} can extend the lifetime and reduce the charging time of Li-ion batteries when compared with the CC-CV charging. However, both studies have not considered the CV phase for the SRC and the PPC charging when compared to the CC-CV charging. This is why some other studies that consider the CV phase into the SRC or PPC charging strategies came to the opposite conclusions [27]. Therefore, it is worth noticing that the pulsed current charging with the CV phase and without the CV phase will have different evaluation results when it was compared with the CC-CV charging. Therefore, the fair way to evaluate the pulsed current charging is to compare it with the CV phase to the CC-CV charging or compare it without the CV phase to the CC charging. If only look into the literature that evaluated the PPC charging in the aforementioned way, most of them have the same conclusions, i.e., the pulsed current has no significant effect on the charging rate and the lifetime of Li-ion batteries [8], [19], [30]. Therefore, the optimal condition of the PPC charging is needed to be investigated.

TABLE I
Existing Studies on the Pulsed Current Charging Techniques And Their Effect on Lifetime of Lithium-ion Batteries. (×: not given; +: positive effect; 0: no significant effect; -: negative effect.)

Ref.	Current mode	Compared to	frequency [Hz]	Lifetime extension	Evaluation
[22]	PPC	CC-CV	12k	+100 cycles	**+**
[18]	SRC	CC-CV	1k	+16.1%	**+**
[19]	SRC	CC	1k, 100, 1	±1.5%	**0**
[27]	PPC-CV	CC-CV	1k	-0.5%	**0**
			100	-12%	**-**
			50	-7.6%	**-**
[28]	PCCC	CC-CV	25	0%	**0**
			1	-2%	**0**
[21]	NPC-CV	CC	0.01	-1.6%	**0**
			0.005	-0.3%	**0**
		CC-CV	0.01	+0.2%	**0**
			0.005	+1.1%	**0**
[25]	NPC-CV	CC-CV	0.046, 0.023	+17.1%	**+**
[20]	NPC	CC-CV	×	+128.6%	**+**

B. Degradation Mechanisms

Li-ion batteries are affected by capacity and power fade during cycling. The performance degradation of Li-ion batteries is related to the loss of lithium inventory (LLI), loss of active material (LAM), and the change in reaction kinetics that indicated an increase of internal resistance (IR) [31]. The formation and growth of solid electrolyte interface (SEI) film are one of the important factors of side reactions, which result in the LLI [32]. The decrease of power capability is caused by

the IR evolution. Generally, a Li-ion battery reached its end of life (EOL) when there is a capacity loss of 20% respected to the initial capacity [33].

The disassembly-based post-mortem analysis, the model-based analysis, and the curve-based analysis are the three methods using to diagnose the aging of Li-ion batteries [34]. The disassembly-based analysis can determine the degradation mechanism by disassembling the aged cell in a special operating environment, and using professional equipment to observe the structure of the electrodes (e.g., atomic force microscopy (AFM) and scanning electron microscopy (SEM) techniques) and analyze the chemical composition changes (e.g., energy dispersive X-ray spectroscopy (SEM-EDX) and X-ray photoelectron spectroscopy (XPS) techniques) of the aging cells [35]. However, this is a destructive method due to the requirement of disassembling the cell and thus ending the cycling aging test. Therefore, the disassembly-based post-mortem analysis is suitable for cross-validation after completing the cycling aging test [34]. The model-based method is using the EIS technique to measure the cell impedance and to obtain the electrochemical model parameters based on the EIS data. The aging process of the cells can be analyzed according to the model parameter evolution [36]. This method is a non-destructive method but needs the equipment which can perform the EIS measurement [34].

The curve-based analysis consists of Incremental Capacity (IC) analysis and differential voltage (DV) analysis, which show how the capacity increment changes with the voltage of the cell. The incremental capacity is determined by the differentiating the change in capacity dQ to the change in terminal voltage dV, i.e., $\frac{dQ}{dV}$. The conclusions obtained by the IC curve and DV curve are overall consistent when analyzing the aging process of batteries because the DV curve is inversely related to the IC curve [34], [37]. The obtaining of the IC curve only needs to perform a charging/discharging cycle by a constant current for batteries and monitor the changes in voltage and current; thus, this method is more suitable for practical applications due to the advantages of non-destructivity and simple implementation [37]. In [38], Dubarry et al. proposed that the degradation of lithium-ion batteries includes two stages by analyzing the evolution of IC curves. The contributions of the three degradation mechanisms, i.e., LLI, LAM, and the change in reaction kinetics, which is indicated as the increase in the IR, are different in the two stages. The first stage of the capacity fade is dominated by LLI, which occurs as a result of parasitic reactions to form the SEI layer on the electrode surfaces. The degradation due to the LLI continues in the second stage. Moreover, as the SEI layer continues to evolve on the electrode surfaces, it hinders interfacial kinetics and induces LAM in both electrodes. Moreover, when the SEI layer grows too thick, some grains will be isolated and become inactive, resulting in LAM [31]. Therefore, the three main degradation mechanisms occur together and accelerate the capacity fade in the second stage [38]. However, 20% capacity fade is not the sign which indicates that the battery reached the second stage. The typical characteristic of the battery in the second stage is an accelerated capacity degradation compared to that of the first stage. Moreover, the battery has started entering the second stage before showing the accelerated capacity fade [38]. Therefore, the effect of different charging currents on battery lifetime can be analyzed through the changes in the stage of Li-ion batteries.

TABLE II
SPECIFICATIONS OF THE TESTED CELLS.

Parameter	Value
Model	HTCNR18650
Format	Cylindrical cell
Chemical system	NMC
Nominal capacity, Cap_n	2,200 mAh
Nominal voltage, V_n	3.6 V
Charging cut-off voltage, V_{max}	4.2 V
Discharging cut-off voltage, V_{min}	2.5 V
Maximum (dis)charging current, I_{max}	3 C (6.6 A)

C. Summary

The effects of various pulsed current charging on the lifetime of Li-ion batteries have been investigated in the literature. However, the previous work focused on the frequency above 1 Hz and seldom mentioned the frequency below 1 Hz for the PPC charging. This paper investigated low-frequency PPC charging and its effects on the lifetime of Li-ion batteries. Moreover, the effects of the pulsed current on the different degradation stages are analyzed by a degradation model of Li-ion batteries. The main contributions of this paper are summarized as follows:

(1) Through the experimental testing, it is observed that the PPC charging at low frequencies can extend the lifetime of Li-ion batteries by 69.2% when compared with the traditional CC charging, which provides guidance for selecting the frequency range of the pulsed current charging.
(2) By developing a two-stage degradation model, the effects of the frequency on the three main degradation mechanisms, i.e., LLI, LAM, and kinetics hindrance, at different aging stages are determined.
(3) With IR evolution and IC curve analysis, the effects of pulsed current charging on the degradation of Li-ion batteries are comprehensively explored.

Moreover, the changes in the maximum rising temperature and the energy efficiency during the aging process, which are caused by the CC and PPC charging, are used to investigate the effects of the pulsed current on the charging performances of Li-ion batteries.

III. EXPERIMENT

The experimental investigations on PPC charging were performed using a Digatron battery test station. The test error of the voltage and current using this equipment is smaller than 0.025%. A Memmert temperature chamber is used to maintain a stable and reliable temperature during all tests, as shown in Fig. 1(a). The cylindrical NMC-based HTCNR18650 2200-mAh cells are used for performing these investigations. The

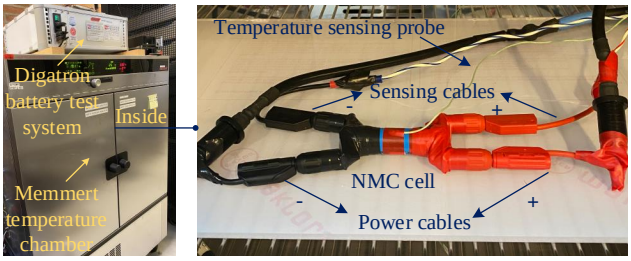

Fig. 1. (a) Experimental setup and (b) an NMC cell is placed in the temperature chamber during the test.

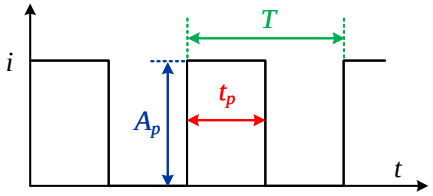

Fig. 2. Positive pulsed current (PPC).

specifications of the cells are summarized in Table II. Fig. 1(b) shows a battery cell is during the test.

The waveform of the PPC is presented in Fig. 2, where T is the period of the PPC; A_p is the amplitude of the pulses; t_p and t_r are the duration of the positive pulsed current and the relaxation period, respectively. The frequency f and the duty cycle D of the PPC charging are defined as follows:

$$f = \frac{1}{T} \tag{1}$$

$$D = \frac{t_p}{T} \tag{2}$$

The CC charging is regarded as the reference to evaluate the PPC charging. The cells are charged by the PPC or the CC until the voltage reaches the maximum voltage V_{max}. The flowchart of the experimental procedures is presented in Fig. 3.

In the cycle aging test, the frequencies of the PPC charging are 1 Hz, 0.2 Hz, and 0.05 Hz with a duty cycle of 50%. The average current of the PPC charging is the same as that of the CC charging. The amplitude of the PPC charging is 2 C, while the amplitude of the CC charging is 1 C. After completing every charging process, the cells were discharged by a CC of 2 C. All cells were performed 1000 cycles. To speed up the capacity degradation of the cells, the temperature of the climate chamber was set at 35 °C.

The reference performance tests were performed before the cycling procedure was started, and then after every 100 cycles of the aging test. The reference performance tests consist of the capacity test, IR test, and IC test. The temperature of the climate chamber was set at 25 °C during the reference performance tests.

To obtain the cell's capacity, the cell is fully charged with 1-C CC-CV and relaxed for one hour; then the cell is fully discharged with 1-C CC. The obtained discharging capacity is considered as the capacity of the cell.

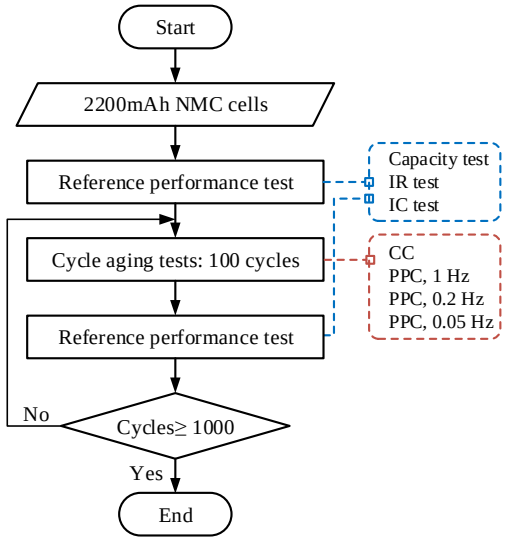

Fig. 3. Experimental procedures.

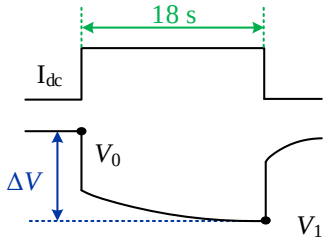

Fig. 4. DC pulse for IR measurement.

The IR was measured using the Direct Current (DC) pulse technique at different SOCs. The following procedure is repeated for IR measurement for 10%, 30%, 50%, 70%, and 90% SOCs [39], [39], [40]:

1) Charge the battery cell to the desired SOC;
2) Relax the battery cell for 15 minutes at 25 °C;
3) Discharge the battery cell by using a 1-C current pulse for 18 seconds;
4) Relax the battery cell for 15 minutes at 25 °C;
5) Charging the battery cell by using a 1-C current pulse for 18 seconds;
6) Repeat steps 1-5 for the other SOCs.

Fig. 4 shows an example of the IR measurement by DC pulse. The internal resistance IR of the cell can be determined using Ohm's law as follows:

$$IR = \frac{V_0 - V_1}{I_{dc}} = \frac{\Delta V}{I_{dc}} \tag{3}$$

where V_0 and V_1 are the voltage before and after the 18-seconds DC pulse I_{dc}; ΔV is the voltage change caused by the DC pulse. The average of positive and negative resistances was considered as cells' IR at corresponding SOCs.

A constant current of 0.04 C is suggested for performing the IC test because this low current rate can avoid the effect of the polarization resistance of the batteries on IC curves. However, 50 hours are needed for the charging/discharging cycle if 0.04 C is used. This is not suitable for real applications with such

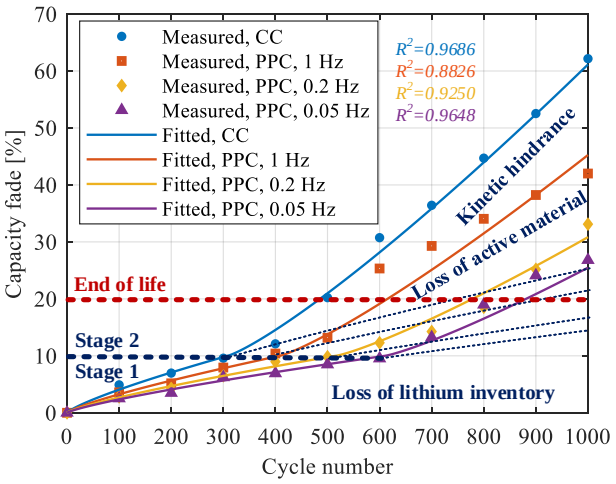

Fig. 5. Measured and fitted capacity fade of the tested cells that were cycled with the CC and PPC charging.

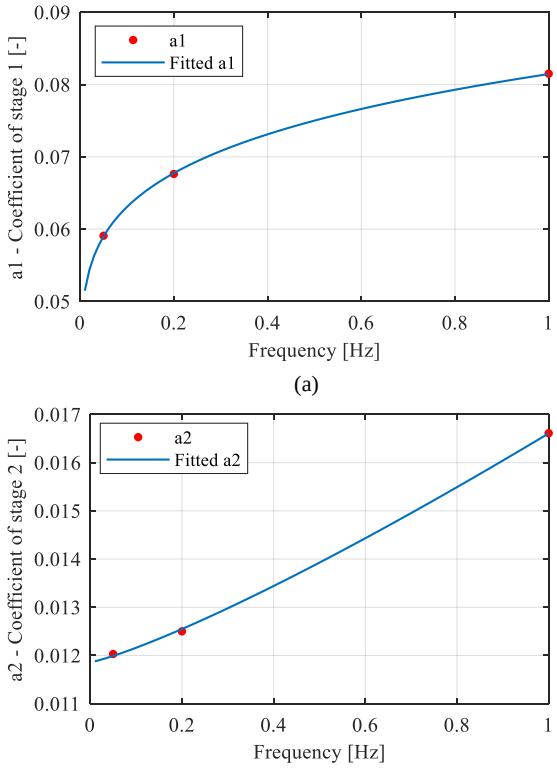

Fig. 6. Relationship between the frequency coefficient and the fre-quency: (a) the frequency coefficient at stage 1 a1(f) and (b) the frequency coefficient at stage 2 a2(f).

a long period. Moreover, the main changes in the behavior of the IC curve can be observed with a current rate that is higher than 0.04 C [41]. In [37], it is reported that the current rate that is lower than 0.5 C can meet the requirement of obtaining the effective IC curve to analyze the degradation mechanism of Li-ion batteries by comparing the effect of different current rates on IC curves. Therefore, the IC test was performed with a current rate of 0.2 C, i.e., 0.44 A. The other issue needed to be considered for the IC test is the sampling frequency. In [37], it illustrated that the sampling rate shouldn't be lower than 0.1 Hz; otherwise, it will impact the magnitude and the position of the peaks of IC curves; however, the IC curve with a sampling frequency that is higher than 1 Hz will not provide extra information on IC behavior. Therefore, the sampling frequency of the IC test is 1 Hz in this work.

IV. Results And Discussion

A. Capacity Fade

Fig. 5 shows the capacity fade of the NMC battery cells that were cycled by the CC and PPC charging. After 500 cycles, the capacity fade of the cell that was cycled with the CC charging is 20.21%, which means the cell reached its EOL. In contrast, the cells that were cycled with PPC charging at the frequencies of 1 Hz, 0.2 Hz, and 0.05 Hz reach their EOL after 600 cycles, 900 cycles, and 900 cycles, respectively. Moreover, a lower frequency of the PPC charging results in a lower capacity fade within the considered frequency range after 1000 cycles.

Accelerated capacity fade can be observed at specific cycle numbers, e.g., the 400th cycle of the CC charging. This means the battery cell is already in the second stage of the aging process. The exact starting point of the second aging stage can be determined by disassembling the battery and then using professional instruments to observe and analyze the aging mechanism of the battery. This method is a destructive method for the requirement of disassembling the cell and is not suitable for this work to analyze the aging mechanism. This work defines the boundary of the two stages by analyzing the changes in the capacity fade rate of the battery during the cycling process.

The second stage of the battery degradation is earlier than that the accelerated capacity fade occurs. Therefore, the battery cell that was aged by the CC charging started the second stage before 400 cycles, i.e., around the 300th cycle. After 300 cycles, the capacity fade of the cell using the CC charging is 10%; thus, the capacity fade of 10% is regarded as the boundary of the change in the degradation mechanism.

The battery cells that were cycled by the PPC charging at 1 Hz, 0.2 Hz, and 0.05 Hz reach 10% capacity fade after 400 cycles, 500 cycles, and 600 cycles, respectively. To analyze how the PPC charging affects the battery lifetime at different stages, a piecewise power function was considered to fit the capacity fade as follows:

$$\begin{cases} Q_{fade.s1}(N)[\%] = a_1(f) \cdot N^{0.8}, & when\ Q_{fade} \leq 10\% \\ Q_{fade.s2}(N)[\%] = a_2(f) \cdot (N - N_{s1})^{1.2} + 10, & when\ Q_{fade} > 10\% \end{cases} \tag{4}$$

where N is the cycle number; N_{s1} is the cycle number when the capacity fade reached 10%, i.e., before starting the second aging stage; $Q_{fade.s1}$ and $Q_{fade.s2}$ are the capacity fade of the battery cell at stage 1 and stage 2, respectively; a_1 and a_2 are the fitting coefficient of stage 1 and stage 2, respectively. The accuracy of the fitting results was quantified by the R^2 coefficient. The relationship between the coefficient, i.e., $a_1(f)$ and $a_2(f)$, and the frequency were found and are given by:

$$a_1(f) = 0.04978 \cdot f^{0.2} + 0.03167 \tag{5}$$

$$a_2(f) = 0.004746 \cdot f^{1.2} + 0.01186 \tag{6}$$

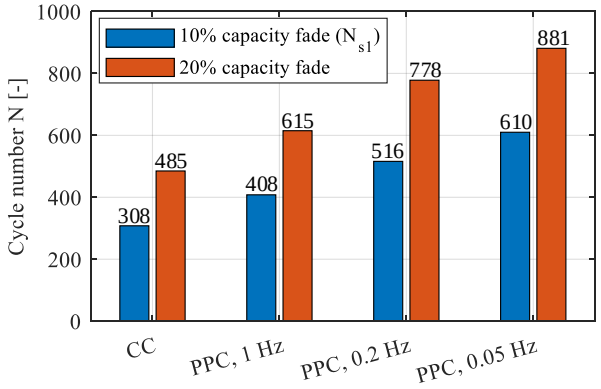

Fig. 7. Cycle numbers of the tested battery cells when the capacity fade reached 10% and 20% based on the proposed degradation model.

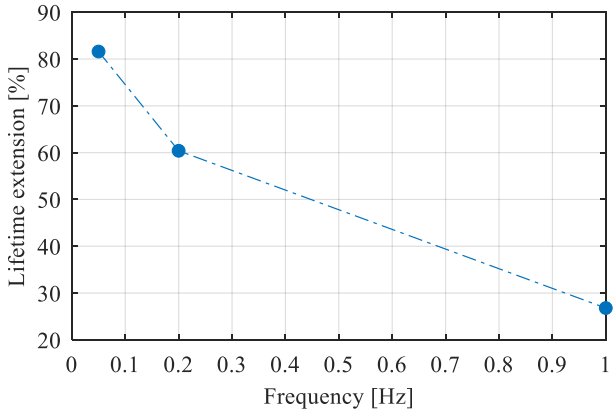

Fig. 8. Lifetime extension by the PPC charging with respect to the standard CC charging.

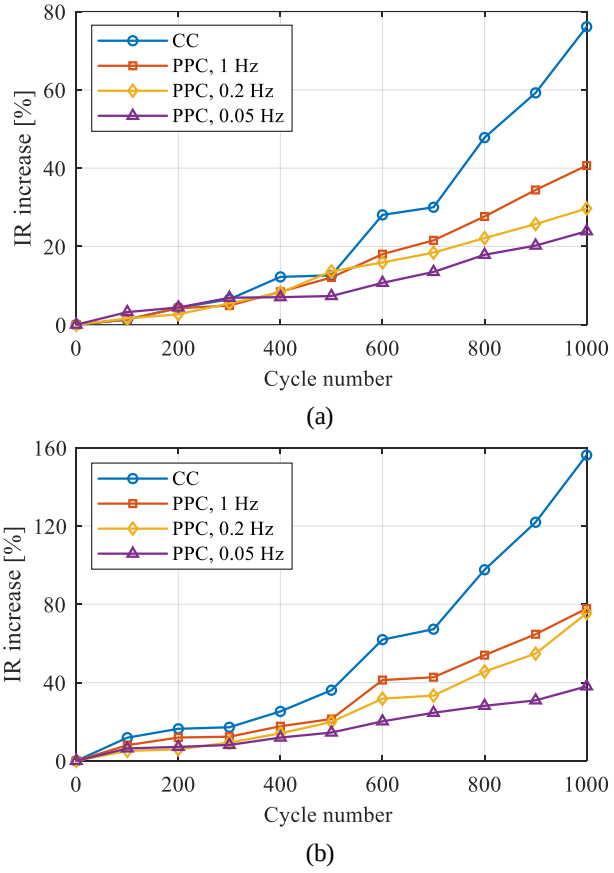

Fig. 9. Percentage increase in the internal resistance (IR) during cycling: (a) SOC=10% and (b) SOC=50%.

For the CC charging, the degradation model can also be expressed as (4). The values of the coefficients a_1 and a_2 for the CC charging are 0.102 and 0.01998, respectively.

The coefficients a_1 and a_2 can be used to describe the rate of the capacity fade. Fig. 6 presents the dependence, on the frequency of the pulsed current, of the coefficients at stage 1 $a_1(f)$ and stage 2 $a_2(f)$. The value of the red dashed line is the coefficient of the CC charging. The red dashed line is used to compare the coefficient of CC charging with the PPC charging with different frequencies, while the frequency has no substantial meaning for the CC charging. The PPC charging at the considered frequency range can slow down the capacity fade at both stage 1 and stage 2 when compared with the CC charging. In Fig. 6(a), the changes in the coefficient $a_1(f)$ at the frequency range between 0.05 Hz and 1 Hz are significant, which means the degradation of the battery cell at stage 1 is considerable influenced by the frequency of the pulsed current. In Fig. 6(b), the coefficient $a_2(f)$ at 0.2 Hz and 0.05 Hz are almost the same, but they are much lower than that of at 1 Hz. Therefore, the impact on battery degradation at stage 2 is not significant with the frequency decrease.

According to the proposed degradation model in (4), the cycle numbers can be obtained when the capacity fade reached 10% and 20%, as shown in Fig. 7. It can be observed that the PPC charging can inhibit battery degradation during both stages. The PPC charging at 1 Hz, 0.2 Hz, and 0.05 Hz can slow down the rate of the battery degradation by 32.5%, 67.5%, and 98.1% during the first 10% capacity fade; after the second 10% capacity fade, the PPC charging at the considered frequencies can slow down the degradation rate of the battery by 26.8%, 60.4%, and 81.6%, respectively. Therefore, the PPC charging positively impacts the battery lifetime during the second 10% capacity fade, but this effect is slightly weaker than the first 10% capacity fade. A 20% capacity fade is considered as the EOL of the battery cell. The extension of each PPC charging case is presented in Fig. 8.

B. Internal Resistance

The IR is quasi-independent on SOC for SOCs between 30% and 90%, independent on the aging state; thus, the IR at 50% is presented in the following part to represent that of this SOC range. Figs. 9(a) and (b) show the percentage increases in IR at 10% SOC and 50% SOC. It can be observed that the IR evolution at 10% SOC is slower than that of 50% SOC for all cells. However, both of them show the same increasing trend. During the aging test, the CC charging results in a much faster IR increase than the PPC charging. Furthermore, the smaller frequency leads to a slower degradation ratio of the IR, which is consistent with the results of capacity fade.

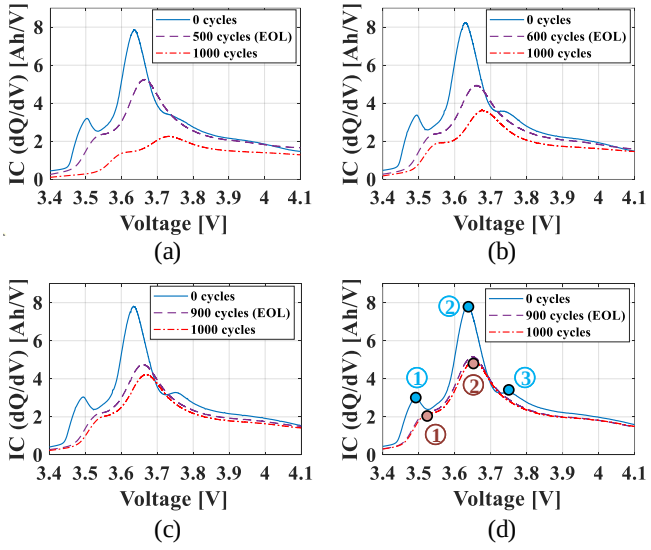

Fig. 10. Incremental capacity (IC) curves before the cycling aging test, at EOL, and after 1000 cycles: (a) CC, (b)-(d) PPC at 1 Hz, 0.2 Hz, and 0.05 Hz, respectively.

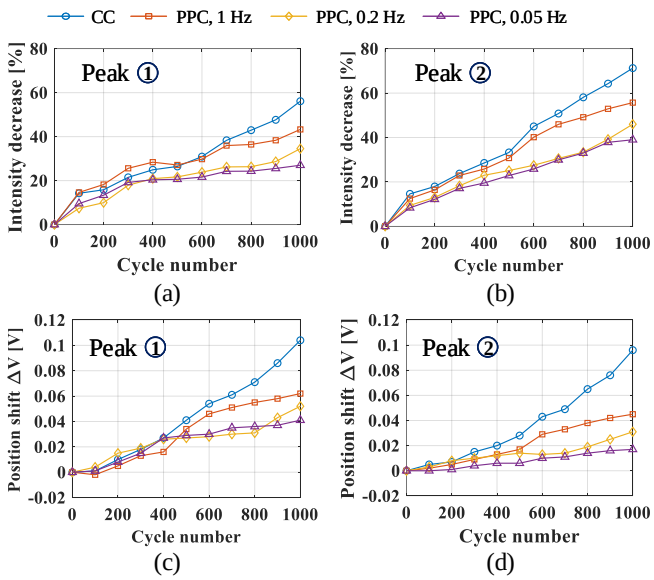

Fig. 11. Changes in IC curves: (a) and (b) are the decrease in intensity of peak ① and ②, (c) and (d) are the shift in position of peak ① and ②.

C. Incremental Capacity

Fig. 10 presents the IC curves at different aging states of the four tested cells. In Figs. 10(a)-(d), the three IC curves of each figure are obtained when cells were fresh, cells reached their EOL, and cells have performed 1000 aging cycles, respectively. There are three peaks, i.e., peak ①, peak ②, peak ③ on the initial IC curves. The intensity of peak ① and peak ② decrease when the cells reached their EOL, and further decrease after completing 1000 cycles. Moreover, the position of peak ① and peak ② shift to a higher voltage after 1000 cycles when compared with their initial voltage positions. Besides, the peak ③ is disappeared for all cells after the aging tests.

Fig. 11 shows the percentage decrease in the intensity and the shift in the voltage position of peaks ① and ②. The intensity of peaks ① and ② decreases with increasing the number of cycles. Moreover, the cell with a faster capacity fade shows a higher intensity decrease and a larger voltage position shift for both peaks ① and ② during the cycling.

D. Analysis of Degradation Mechanisms

The decrease in intensity of peak ② and the battery capacity fade show a similar evolution trend because they are directly related to each other. Before the capacity fade reaches 10%, the main degradation mechanism is LLI, which occurs as a result of parasitic reactions to form the SEI layer on the electrode surfaces. Therefore, the cell that was cycled with the PPC can slow down the capacity fade by inhibiting SEI layer growth during stage 1. Moreover, the PPC with a lower frequency in the investigated frequency range can further enhance this inhibiting effect. In Fig. 6(a), the significant difference in coefficient a_1 illustrated that both the pulsed current and frequency can influence the battery degradation mechanism in the first stage. During stage 2, the three degradation mechanisms, i.e., LLI, LAM, and kinetic hindrance, occurred together, thereby leading to the intensified capacity degradation of the battery cells. The capacity fade from the LLI still follows the same increased fashion as stage 1, as the blue dashed line shown in Fig. 5. The area between the blue dashed line and the x-axis is the capacity degradation caused by LLI. The area between the blue dashed line and the corresponding solid line (i.e., the fitted capacity fade curve) is the capacity fade by the LAM and the kinetic hindrance. According to the size of the area, the pulsed current in the second stage can not only continue to suppress the capacity degradation caused by LLI but also inhibit the capacity degradation caused by LAM and kinetic factors. Different from stage 1, the suppression of the LAM and kinetic factors by the PPC charging will not continue to be strengthened as the frequency decreases during stage 2. In Fig. 6(b), the values of a_2 at 0.2 Hz and 0.05 Hz are close to each other. Thus, the PPC charging at 0.2 Hz and 0.05 Hz has a similar impact on the LAM and kinetic hindrance during stage 2.

The shift in the position of peaks ① and ② is another significant change during cycling. The increase in the IR is the main reason resulting in the peak shift [19], [37], [38], [42]. The peak shift leads to a less effective charging process when the cell voltage gradually approaching the charging cut-off voltage V_{max}. This phenomenon is also called undercharging (UC) since a greater available capacity can be obtained by setting a higher charging cut-off voltage [42]. However, typically, the charging cut-off voltage in IC tests as well as in normal charging/discharging cycles is constant, thus the accelerated capacity fade will be observed as we aforementioned. According to the results shown in Figs. 11(c)-(d) and Fig. 9, the increase in the IR and the position shift in peaks of IC curves have a consistency.

In Fig. 10, the broadening of the peaks on IC curves can be observed, especially peak ①, which is at the low voltage position. During cycling, the SEI could be partly

dissolved, and the graphite would result in an amorphous state [31], [43]. Therefore, the SEI destabilization and disorder of graphite surface results in the peak broadening [31]. Peak ③ can be considered as the shoulder of the IC curve, which is disappeared when the increased IR prevents the phase transitions from occurring at the initial voltage position [34]. Therefore, the phenomenon of the peak broadening and the disappearance of the peak is also the aging sign for Li-ion batteries.

E. Maximum Rising Temperature

The temperatures of the battery cells were measured during the entire experiment. The maximum rising temperature ΔT is the difference between the initial temperature $T_{init.}$ and the maximum temperature $T_{max.}$ of the battery cell during the charging process:

$$\Delta T = T_{max.} - T_{init.} \tag{7}$$

Fig. 12 shows the maximum rising temperature of the cells that were aged by different current. For example, the three maximum rising temperatures of the CC case in Fig. 12 were obtained at the 1^{st}, the 501^{st}, and the 1000^{th} cycle numbers. When cells were fresh, the maximum rising temperature of CC charging and the PPC charging at 1 Hz, 0.2 Hz, 0.05 Hz are 2.8 °C, 2.9 °C, 3.1 °C, and 3.3 °C, respectively. Therefore, the PPC charging results in a higher rising temperature at the begin of lifetime of the cells. Similar thermal performance of the PPC charging has been reported in our previous work [44]. With the increasing cycle number, the maximum rising temperature of all cells gradually increases during cycling due to the increase in the IR, which results in more heat losses.

At the 1000th cycle, the maximum rising temperatures of the cells charged by the CC, 1-Hz PPC, 0.2-Hz PPC, and 0.05-Hz PPC charging are 8.6 °C, 5.5 °C, 5.1 °C, and 5.2 °C, respectively. This means the PPC charging can reduce the maximum rising temperature by 60.5% compared to the CC charging. In Fig. 9, after the entire aging test, the lower IR evolution of the battery cell is obtained by using the PPC charging, which can reduce the heat losses, thereby showing a lower rising temperature compared with the CC charging. Therefore, as the degree of battery degradation increases, the increase in IR is the main factor that results in the high rising temperature during the charging process.

F. Energy Efficiency

The energy efficiency represents the losses during one charging/discharging cycle. The energy efficiency is obtained from the life cycle test, where the cells were charged by the CC or the PPC and discharged by a constant current of 2 C. Due to the same discharging procedure, the difference in the energy efficiency of the fresh cells can be attributed to the different charging currents. The energy efficiency η_E is determined as:

$$\eta_E = \frac{Energy_{dis}}{Energy_{cha}} \times 100\% \tag{8}$$

where $Energy_{cha}$ and $Energy_{dis}$ are the charging energy and discharging energy, respectively.

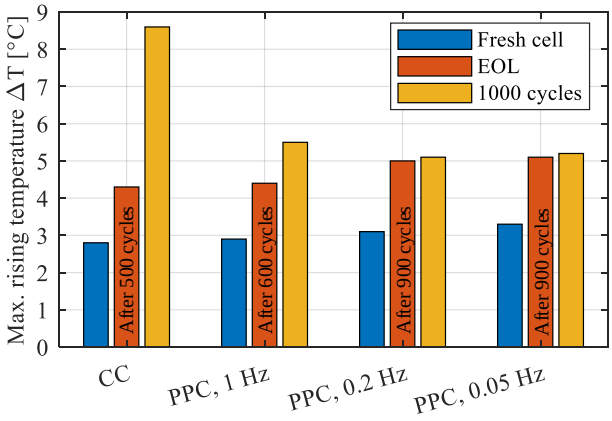

Fig. 12. Maximum rising temperature of the battery during the charging process.

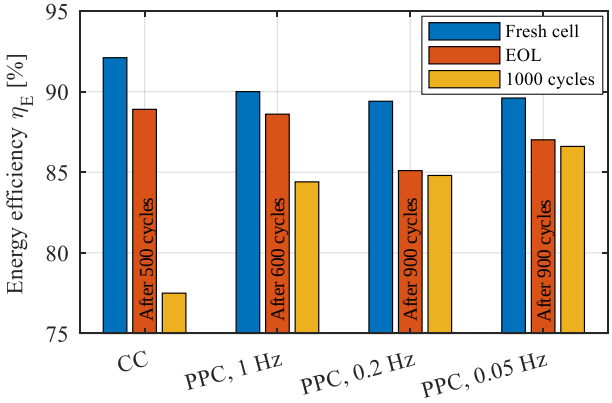

Fig. 13. Energy efficiency of one cycle of discharging with a constant current of 2.2 A and charging with the CC charging and the PPC charging at different frequencies.

The obtained energy efficiency of the four test conditions is presented in Fig. 13. When cells were fresh, the energy efficiency for the CC charging is 92.1%, while the energy efficiency for the PPC charging at 1 Hz, 0.2 Hz, and 0.05 Hz are 89.9%, 89.3%, and 89.5%, respectively. Therefore, the difference in the energy efficiency for the PPC charging with different frequencies is within 0.6%, but they are all lower than the energy efficiency of the CC charging by 2.2% above. Therefore, the heat losses of the cells charged by the PPC are higher than that of the CC. After 1000 cycles, the energy efficiencies for the CC and PPC at 1 Hz, 0.2 Hz, and 0.05 Hz are 77.5%, 84.4%, 85.1%, and 86.6%, respectively, which are significantly lower than their initial energy efficiencies. This means that the heat losses generated during both charging and discharging processes increases due to the increase in IR of four cells. Therefore, the lowest energy efficiency and the highest energy efficiency are obtained from the cells that were cycled by the CC charging and 0.05-Hz PPC charging, which are corresponding the highest IR and the lowest IR, respectively. The energy efficiency resulted from the PPC charging is higher than that of CC charging by 9.1% after 1000 cycles.

V. Conclusion

The effect of low-frequency PPC charging on the lifetime of NMC-based battery cells has been investigated in this paper. A two-stage degradation model is developed to analyze the effect of the PPC charging on the degradation mechanisms at different stages. During stage 1, the PPC charging can reduce the LLI by inhibiting the SEI layer growth. Moreover, a lower frequency of the PPC charging can further enhance this inhibiting effect, thereby slowing down the process of the battery cells entering the second stage. During stage 2, the PPC charging can slow down the battery degradation by restraining the LLI, LAM, and kinetic hindrance. The PPC charging at 0.2 Hz and 0.05 Hz have a similar impact on the degradation mechanisms of LAM and kinetic hindrance. Therefore, the difference in capacity fades between 0.2-Hz PPC charging and 0.05-Hz PPC charging mainly results from their influence on the LLI of the battery cells. Based on the experimental results and the degradation model, the PPC charging at 1 Hz, 0.2 Hz, and 0.05 Hz can extend the battery lifetime by 26.8%, 60.4%, and 81.6%, respectively, when compared with the CC charging. When battery cells were fresh, no evidence indicated that the PPC charging has advantages on cell temperature and energy efficiency. After 1000 cycles, the maximum rising temperature and energy efficiency of the Li-ion battery cells that were cycled by the PPC charging at 0.05 Hz are improved by 60.5% and 9.1%, respectively, when compared with the CC charging. Finally, the PPC charging at 0.05 Hz shows the best lifetime extension performance for the NMC-based battery cell within the considered frequency range. Therefore, low-frequency PPC charging should be considered as a promising charging strategy to satisfy the future requirements of fast charging and lifetime extension for Li-ion batteries.

References

[1] T. Or, S. W. D. Gourley, K. Kaliyappan, A. Yu, and Z. Chen, "Recycling of mixed cathode lithium-ion batteries for electric vehicles: Current status and future outlook," *Carbon Energy*, vol. 2, no. 1, pp. 6–43, Jan. 2020.

[2] Y. Wu, S. Zhang, J. Hao, H. Liu, X. Wu, J. Hu, M. P. Walsh, T. J. Wallington, K. M. Zhang, and S. Stevanovic, "On-road vehicle emissions and their control in china: A review and outlook," *Science of The Total Environment*, vol. 574, pp. 332–349, Jan. 2017.

[3] N. Rietmann and T. Lieven, "How policy measures succeeded to promote electric mobility – worldwide review and outlook," *J. Cleaner Production*, vol. 206, pp. 66–75, Jan. 2019.

[4] Y. Yao, Z. Wei, H. Wang, H. Huang, Y. Jiang, X. Wu, X. Yao, Z.-S. Wu, and Y. Yu, "Toward high energy density all solid-state sodium batteries with excellent flexibility," *Advanced Energy Materials*, vol. 10, no. 12, p. 1903698, Mar. 2020.

[5] Y. Jin, K. Liu, J. Lang, X. Jiang, Z. Zheng, Q. Su, Z. Huang, Y. Long, C. an Wang, H. Wu, and Y. Cui, "High-energy-density solid-electrolyte-based liquid li-s and li-se batteries," *Joule*, vol. 4, no. 1, pp. 262–274, Jan. 2020.

[6] H. Li, X. Zhang, J. Peng, J. He, Z. Huang, and J. Wang, "Cooperative CC–CV charging of supercapacitors using multicharger systems," *IEEE Trans. Ind. Electron.*, vol. 67, no. 12, pp. 10 497–10 508, Dec. 2020.

[7] L. K. Maia, L. DrÃ¼nert, F. L. Mantia, and E. Zondervan, "Expanding the lifetime of li-ion batteries through optimization of charging profiles," *J. Cleaner Production*, vol. 225, pp. 928–938, Jul. 2019.

[8] S.-Y. Cho, I.-O. Lee, J.-I. Baek, and G.-W. Moon, "Battery impedance analysis considering DC component in sinusoidal ripple-current charging," *IEEE Trans. Ind. Electron*, vol. 63, no. 3, pp. 1561–1573, Mar. 2016.

[9] A. S. Mussa, M. Klett, M. Behm, G. Lindbergh, and R. W. Lindstrom, "Fast-charging to a partial state of charge in lithium-ion batteries: A comparative ageing study," *J. Energy Storage*, vol. 13, pp. 325–333, Oct. 2017.

[10] Y. Liu, Y. Zhu, and Y. Cui, "Challenges and opportunities towards fast-charging battery materials," *Nature Energy*, vol. 4, no. 7, pp. 540–550, Jun. 2019.

[11] M. Xu, R. Wang, B. Reichman, and X. Wang, "Modeling the effect of two-stage fast charging protocol on thermal behavior and charging energy efficiency of lithium-ion batteries," *J. Energy Storage*, vol. 20, pp. 298–309, Dec. 2018.

[12] C.-H. Lee, M.-Y. Chen, S.-H. Hsu, and J.-A. Jiang, "Implementation of an SOC-based four-stage constant current charger for li-ion batteries," *J. of Energy Storage*, vol. 18, pp. 528–537, Aug. 2018.

[13] L. Jiang, Y. Li, Y. Huang, J. Yu, X. Qiao, Y. Wang, C. Huang, and Y. Cao, "Optimization of multi-stage constant current charging pattern based on taguchi method for li-ion battery," *Applied Energy*, vol. 259, p. 114148, Feb. 2020.

[14] X. Sui, S. He, S. B. Vilsen, J. Meng, R. Teodorescu, and D.-I. Stroe, "A review of non-probabilistic machine learning-based state of health estimation techniques for lithium-ion battery," *Appl. Energy*, vol. 300, p. 117346, Oct. 2021.

[15] K. Liu, X. Hu, H. Zhou, L. Tong, D. Widanalage, and J. Marco, "Feature analyses and modelling of lithium-ion batteries manufacturing based on random forest classification," *IEEE/ASEM Trans. Mechatronics*, pp. 1–1, 2021.

[16] Z. Hua, Z. Zheng, M.-C. Péra, and F. Gao, "Remaining useful life prediction of PEMFC systems based on the multi-input echo state network," *Appl. Energy*, vol. 265, p. 114791, May. 2020.

[17] J. Meng, L. Cai, D.-I. Stroe, X. Huang, J. Peng, T. Liu, and R. Teodorescu, "An automatic weak learner formulation for lithium-ion battery state of health estimation," *IEEE Trans. Ind. Electron.*, pp. 1–1, 2021.

[18] L.-R. Chen, S.-L. Wu, D.-T. Shieh, and T.-R. Chen, "Sinusoidal-ripple-current charging strategy and optimal charging frequency study for li-ion batteries," *IEEE Trans. Ind. Electron.*, vol. 60, no. 1, pp. 88–97, Jan. 2013.

[19] A. Bessman, R. Soares, O. Wallmark, P. Svens, and G. Lindbergh, "Aging effects of AC harmonics on lithium-ion cells," *J. Energy Storage*, vol. 21, pp. 741–749, Feb. 2019.

[20] J. Li, E. Murphy, J. Winnick, and P. A. Kohl, "The effects of pulse charging on cycling characteristics of commercial lithium-ion batteries," *J. Power Sources*, vol. 102, no. 1-2, pp. 302–309, Dec. 2001.

[21] M. A. Monem, K. Trad, N. Omar, O. Hegazy, B. Mantels, G. Mulder, P. V. den Bossche, and J. V. Mierlo, "Lithium-ion batteries: Evaluation study of different charging methodologies based on aging process," *Appl. Energy*, vol. 152, pp. 143–155, Aug. 2015.

[22] J. Amanor-Boadu, A. Guiseppi-Elie, and E. Sánchez-Sinencio, "The impact of pulse charging parameters on the life cycle of lithium-ion polymer batteries," *Energies*, vol. 11, no. 8, p. 2162, Aug. 2018.

[23] J. M. Amanor-Boadu and A. Guiseppi-Elie, "Improved performance of li-ion polymer batteries through improved pulse charging algorithm," *Applied Sciences*, vol. 10, no. 3, p. 895, Jan. 2020.

[24] X. Huang, Y. Li, A. B. Acharya, X. Sui, J. Meng, R. Teodorescu, and D.-I. Stroe, "A review of pulsed current technique for lithium-ion batteries," *Energies*, vol. 13, no. 10, p. 2458, May. 2020.

[25] M. Abdel-Monem, K. Trad, N. Omar, O. Hegazy, P. V. den Bossche, and J. V. Mierlo, "Influence analysis of static and dynamic fast-charging current profiles on ageing performance of commercial lithium-ion batteries," *Energy*, vol. 120, pp. 179–191, Feb. 2017.

[26] F. Savoye, P. Venet, M. Millet, and J. Groot, "Impact of periodic current pulses on li-ion battery performance," *IEEE Trans. Ind. Electron.*, vol. 59, no. 9, pp. 3481–3488, Sep. 2012.

[27] D. R. R. Kannan and M. H. Weatherspoon, "The effect of pulse charging on commercial lithium nickel cobalt oxide (NMC) cathode lithium-ion batteries," *J. Power Sources*, vol. 479, p. 229085, Dec. 2020.

[28] P. Keil and A. Jossen, "Charging protocols for lithium-ion batteries and their impact on cycle life—an experimental study with different 18650 high-power cells," *J. Energy Storage*, vol. 6, pp. 125–141, May. 2016.

[29] X. Huang, W. Liu, A. B. Acharya, J. Meng, R. Teodorescu, and D.-I. Stroe, "Effect of pulsed current on charging performance of lithium-ion batteries," *IEEE Trans. Ind. Electron., in press*, 2021.

[30] A. Bessman, R. Soares, S. Vadivelu, O. Wallmark, P. Svens, H. Ekstrom, and G. Lindbergh, "Challenging sinusoidal ripple-current charging of lithium-ion batteries," *IEEE Trans. Ind. Electron.*, vol. 65, no. 6, pp. 4750–4757, Jun. 2018.

[31] M. Dubarry and B. Y. Liaw, "Identify capacity fading mechanism in a commercial LiFePO4 cell," *J. Power Sources*, vol. 194, no. 1, pp. 541–549, Oct. 2009.
[32] F. Yang, D. Wang, Y. Zhao, K.-L. Tsui, and S. J. Bae, "A study of the relationship between coulombic efficiency and capacity degradation of commercial lithium-ion batteries," *Energy*, vol. 145, pp. 486–495, Feb. 2018.
[33] S. Saxena, C. L. Floch, J. MacDonald, and S. Moura, "Quantifying EV battery end-of-life through analysis of travel needs with vehicle powertrain models," *J. Power Sources*, vol. 282, pp. 265–276, May. 2015.
[34] R. Xiong, Y. Pan, W. Shen, H. Li, and F. Sun, "Lithium-ion battery aging mechanisms and diagnosis method for automotive applications: Recent advances and perspectives," *Renewable and Sustainable Energy Reviews*, vol. 131, p. 110048, Oct. 2020.
[35] M. Simolka, J. F. Heger, H. Kaess, I. Biswas, and K. A. Friedrich, "Influence of cycling profile, depth of discharge and temperature on commercial LFP/c cell ageing: post-mortem material analysis of structure, morphology and chemical composition," *J. Applied Electrochemistry*, vol. 50, no. 11, pp. 1101–1117, Sep. 2020.
[36] P. S. Sabet, A. J. Warnecke, F. Meier, H. Witzenhausen, E. Martinez-Laserna, and D. U. Sauer, "Non-invasive yet separate investigation of anode/cathode degradation of lithium-ion batteries (nickel–cobalt–manganese vs. graphite) due to accelerated aging," *J. Power Sources*, vol. 449, p. 227369, Feb. 2020.
[37] Y. Li, M. Abdel-Monem, R. Gopalakrishnan, M. Berecibar, E. Nanini-Maury, N. Omar, P. van den Bossche, and J. V. Mierlo, "A quick on-line state of health estimation method for li-ion battery with incremental capacity curves processed by gaussian filter," *J. Power Sources*, vol. 373, pp. 40–53, Jan. 2018.
[38] M. Dubarry, C. Truchot, B. Y. Liaw, K. Gering, S. Sazhin, D. Jamison, and C. Michelbacher, "Evaluation of commercial lithium-ion cells based on composite positive electrode for plug-in hybrid electric vehicle applications. part II. degradation mechanism under 2c cycle aging," *J. Power Sources*, vol. 196, no. 23, pp. 10 336–10 343, Dec. 2011.
[39] D.-I. Stroe, "Lifetime models for lithium ion batteries used in virtual power plants," in *Department of Energy Technology*. Aalborg University, 2014.
[40] J. R. Belt, "Battery test manual for plug-in hybrid electric vehicles," Tech. Rep., Sep. 2010.
[41] M. Dubarry, C. Truchot, M. Cugnet, B. Y. Liaw, K. Gering, S. Sazhin, D. Jamison, and C. Michelbacher, "Evaluation of commercial lithium-ion cells based on composite positive electrode for plug-in hybrid electric vehicle applications. part i: Initial characterizations," *J. Power Sources*, vol. 196, no. 23, pp. 10 328–10 335, Dec. 2011.
[42] M. Dubarry, V. Svoboda, R. Hwu, and B. Y. Liaw, "Capacity and power fading mechanism identification from a commercial cell evaluation," *J. Power Sources*, vol. 165, no. 2, pp. 566–572, Mar. 2007.
[43] M. Dubarry, B. Y. Liaw, M.-S. Chen, S.-S. Chyan, K.-C. Han, W.-T. Sie, and S.-H. Wu, "Identifying battery aging mechanisms in large format li ion cells," *J. Power Sources*, vol. 196, no. 7, pp. 3420–3425, Apr. 2011.
[44] X. Huang, Y. Li, J. Meng, X. Sui, R. Teodorescu, and D.-I. Stroe, "The effect of pulsed current on the performance of lithium-ion batteries," in *Proc. IEEE ECCE*, pp. 5633–5640, Oct. 2020.